

AN10899

Sensorless single-shunt FOC on LPC2900

Rev. 01 — 16 December 2009

Application note

Document information

| Info | Content |
|-----------------|--|
| Keywords | LPC2900, FOC, SVPWM, SMC, current observer, PMSM, single shunt DC-link |
| Abstract | This application note discusses the implementation of field-oriented control (FOC) for a permanent magnet synchronous motor (PMSM) using space vector pulse width modulation with a single DC-link shunt for current measurement. Both sensed and sensorless operation is demonstrated by implementation of a virtual motor model using a current observer with a slide mode controller. |

Revision history

| Rev | Date | Description |
|-----|----------|------------------|
| 01 | 20091216 | Initial version. |

Contact information

For additional information, please visit: <http://www.nxp.com>

For sales office addresses, please send an email to: salesaddresses@nxp.com

1. Introduction

Control of electronically commutated (EC) motors can be achieved in various ways. The most straightforward control strategy is ‘six-step’ or ‘trapezoidal control’ which sequentially commutates each phase of a brushless direct current (BLDC) motor. Position feedback of the rotor is given by a Hall sensor or encoder interface. In six-step control only two out of three phases are powered. Sensorless control is possible by measuring the induced voltages called back-EMF of the non-powered ‘floating’ phase.

Another type of control is sinusoidal control using space vector pulse width modulation (SVPWM). This type of controller varies the phase currents depending on the rotor angle eliminating the torque ripple of a six-step control. The downside of sinusoidal commutation is that it attempts to control time-varying motor currents with a time intolerant proportional-integral (PI) controller algorithm, and does not account for interactions between the phases. This causes a performance loss at high speeds.

A more advanced approach is field-oriented control (FOC). This technique is discussed in this application note. With this control strategy each phase is driven sinusoidal and permanently powered in a way that the magnetic field inside the motor is regulated to the most optimal value. This application note discusses the implementation of a single shunt DC-link current measurement that reduces hardware costs to a minimum. Phase currents cannot be measured individually at the same time with a single shunt; therefore reconstruction of the aggregated current vector is necessary.

A sensed version of FOC for position feedback of the rotor features an encoder interface. Hall sensors are also applicable by interpolating the rotor angle using a timer. Sensorless operation is also demonstrated by implementation of a virtual motor model using a current observer with a slide mode controller (SMC).

Table 1. Different control and feedback methods

| | Hall | Encoder | Sensorless: Back-EMF measurement | Sensorless: Current measurement |
|------------|------|---------|-------------------------------------|------------------------------------|
| Six-step | ✓ | ✓ | ✓ | ⊘ |
| Sinusoidal | ✓ * | ✓ | ⊘ | ✓ |
| FOC | ✓ * | ✓ | ⊘ | ✓ |

* Angle must be interpolated with a timer.

The LPC2900 is equipped with useful features for motor control applications, which make software implementation of motor control algorithms easier and off-load the CPU.

- The Modulation and Sampling Control Subsystem ensures easy and reliable control of time critical peripherals. It provides a mechanism implemented in hardware for synchronization of the ADC's with the PWM for exact timing of the sample moments.
- In order to use SVPWM in combination with current vector reconstruction the flexibility of the PWM block in the LPC2900 family is used to a full extent. The dual edge PWM registers are equipped with a shadow register to allow an atomic change of the PWM configuration without disturbing the currently generated PWM outputs. Automatic update of the PWM registers reduces CPU overhead.
- Two independent ADC's are used for mutually independent sample times. The signals are sampled in one clock cycle at 4.5 MHz and converted to 10 bit values at a rate of 400 kHz. This narrow sample window is an indispensable feature for FOC.
- The Quadrature Encoder Interface (QEI) monitors the position and velocity, using hardware registers without generating interrupts.
- The LPC2900 family features a zero wait-state tightly coupled memory (TCM) with dedicated instruction and data busses to get maximum performance out of the CPU and still being deterministic.
- The 32-bit processing power of the ARM968 core of the LPC2900 series compensates for the math-intensive FOC and virtual motor model algorithms.

A demonstration board was developed to demonstrate FOC for a PMSM at an inaudible 20 kHz. It implements an LPC2900 with a three-phase power inverter and supports a quadrature encoder interface (QEI) and a hall sensor. Current measurement is done by a single DC-link shunt placed at the end of the DC-chain, in series with the combined phases. The board also supports sensed or sensorless six-step control with back-EMF measurement. This application note discusses the usage of the demonstration board for FOC motor control in QEI and sensorless operation only. The schematics of the board are given in the appendix.

The various topics covered in this application note are as follows:

1. SVPWM
2. Virtual motor
3. Hardware
4. Software

2. SVPWM

2.1 PMSM and BLDC difference

PMSM and Brushless Direct Current (BLDC) motors are both permanent magnet-based motors with the same basic structure, consisting of permanent magnets on the rotor and windings on the stator. The main difference between BLDC and PMSM is the drive signal for which it is designed. A PMSM is designed for a sinusoidal drive, while a BLDC is designed for a trapezoidal drive. The advantage of a sinusoidal driven motor is the minimized torque ripple that results in a much quieter motor, both electrically and mechanically. The current harmonics are in the switching frequency range resulting in a lower audible noise, lower motor core losses and a reduced current peak. The disadvantages are higher switching losses due to an extra phase that has to be powered constantly.

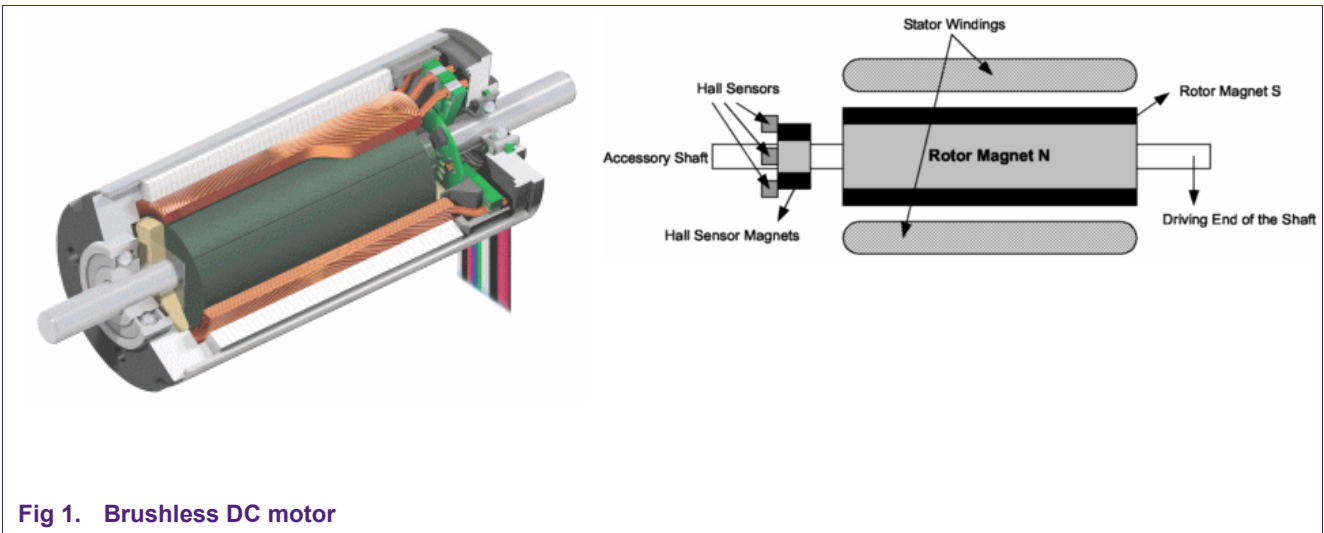


Fig 1. Brushless DC motor

For a sensorless operating BLDC motor, the back EMF has to be trapezoidal. Therefore the rotor is designed to have a uniform flux profile in contrast to the sinusoidal flux profile of a PMSM. A BLDC requires a low winding inductance so it typically uses surface mounted rotor magnets. The high inductance of a PMSM motor makes it less suitable for trapezoidal control.

2.2 FOC basics

The motor in [Fig 1](#) has two main components: stator windings and a permanent magnet. The term synchronous means the magnetic fields generated by the stator and the rotor rotate at the same frequency. In other words PMSM motors do not have the slip that is normally seen in induction motors.

The basic operating theory of FOC is to measure and regulate the magnetic field in the motor. Optimum leverage for the magnetic forces is achieved when the direction of the permanent magnetic field of the rotor is perpendicular to the induced magnetic field of the stator windings. This creates torque on the rotor axis. This principle is illustrated in [Fig 2](#).

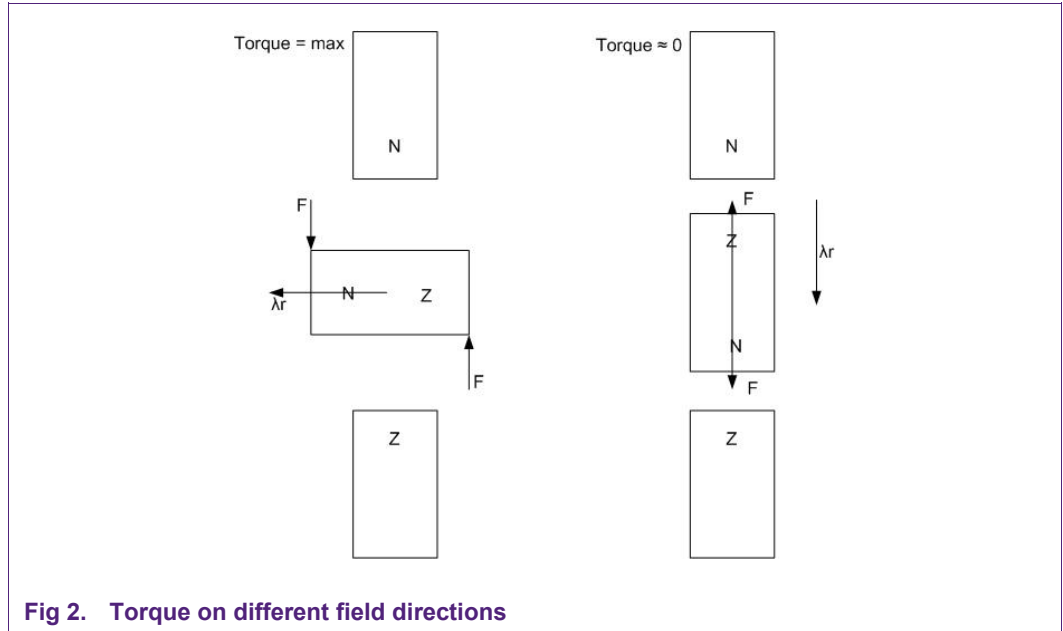


Fig 2. Torque on different field directions

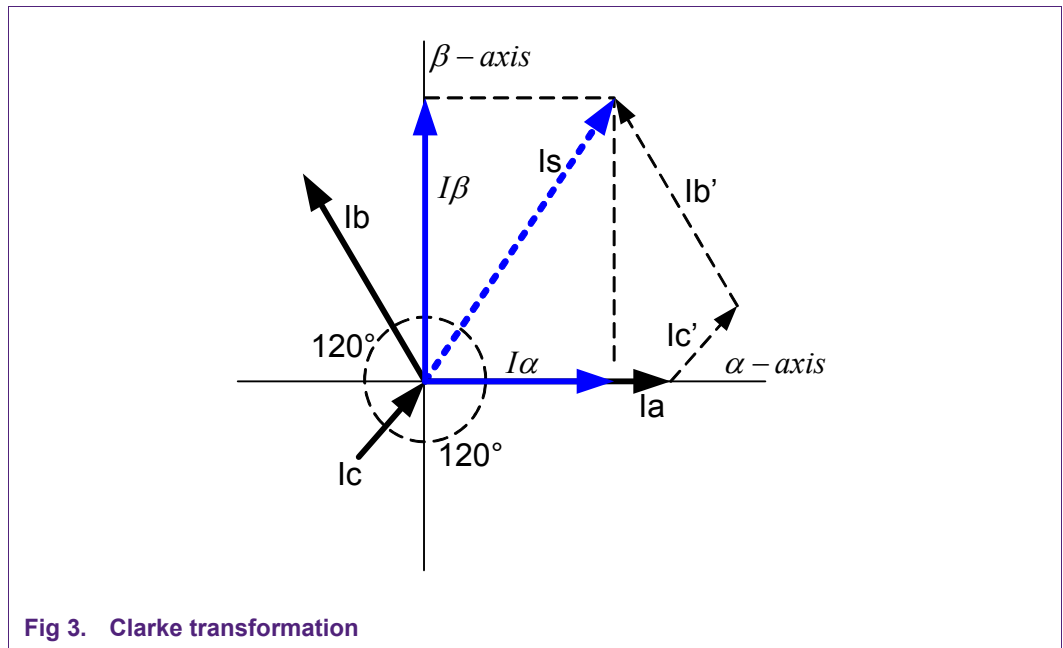


Fig 3. Clarke transformation

The direction and magnitude of the induced magnetic field is equal to the sum of the current vectors of the different phases. Thus by measuring the currents through each phase the total current vector can be calculated. Because the PMSM is a three-phase motor, each phase is separated by 120° .

A 'Clarke transformation' is used to convert a 3-phase system into a 2-phase coordinate system. This frame is called the static reference frame. The quadrature-phase components can be calculated using only two phases of the 3-phase system.

$$I_{\alpha} = I_a - \frac{1}{2}(I_b - I_c) \tag{1}$$

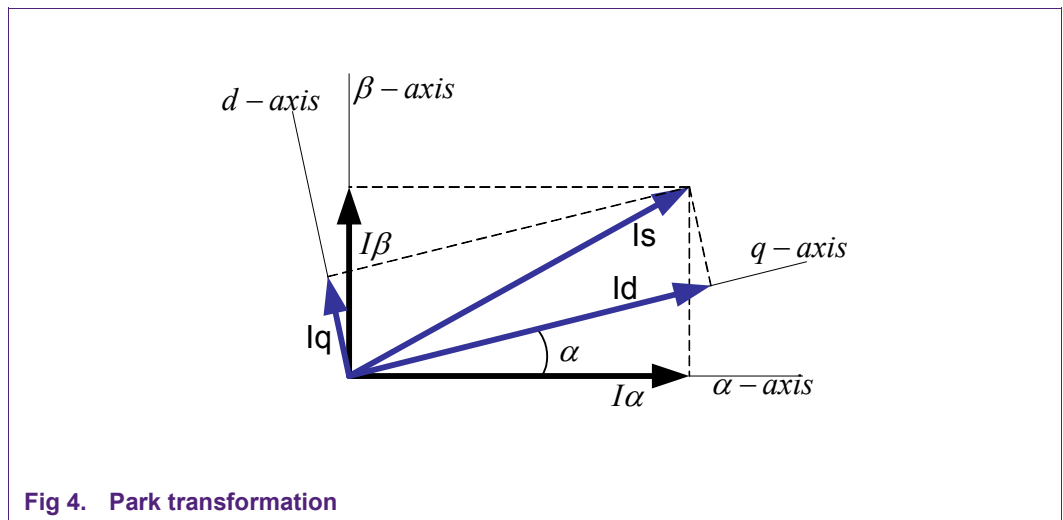
$$I_{\beta} = \frac{1}{2}\sqrt{3}(I_b - I_c) \tag{2}$$

With $I_a + I_b + I_c = 0$ substitution of I_b with $-I_a - I_c$ and scaling with a factor $2/3$ this leads to a non power-invariant transformation:

$$I_{\alpha} = I_a \tag{3}$$

$$I_{\beta} = (I_a + 2 \cdot I_b) / \sqrt{3} \tag{4}$$

The key of FOC is to regulate a magnetic field such that it is perpendicular to the magnetic field of the rotor. By applying a voltage vector to the windings of the motor, the field is controlled. This voltage vector is translated to three duty cycles for each phase by the SVPWM system described in the next paragraph. Both axes of the voltage vector are regulated with a proportional integral (PI) controller. The input of the controller is a single axis of the current vector where the output matches the equivalent axis of the voltage vector. Because the motor spins at high rpm, the field must also spin at the same high frequency. A PI regulator can only be optimally calibrated for a fixed frequency. With the wide speed-range of the motor, an additional step is needed for the PI controller to work optimally. The current vector in the static reference frame (α, β) of the windings can be transformed into the dynamic frame (d, q) of the rotating permanent magnet to create a speed invariant system that can be regulated by a PI controller. A Park transformation is used to transform the static reference frame to a dynamic reference frame. In a zero speed situation, the quadrature component (q) produces torque while the direct component (d) only produces unwanted forces in the motor bearings. For a higher speed range a negative d-component can be used to perform field weakening, which is not covered in this application note.



$$I_d = I_\beta \cdot \sin \alpha + I_\alpha \cdot \cos \alpha \tag{5}$$

$$I_q = I_\beta \cdot \cos \alpha - I_\alpha \cdot \sin \alpha \tag{6}$$

The outputs of the PI controllers are represented as voltage vectors V_q and V_d . An inverse Park transformation is used to go back from the rotating reference frame to the stationary reference frame producing V_α and V_β . Basically it needs to go back to the three-phase currents to control the motor. This technique is called Space Vector Pulse Width Modulation (SVPWM) described in paragraph 2.3.

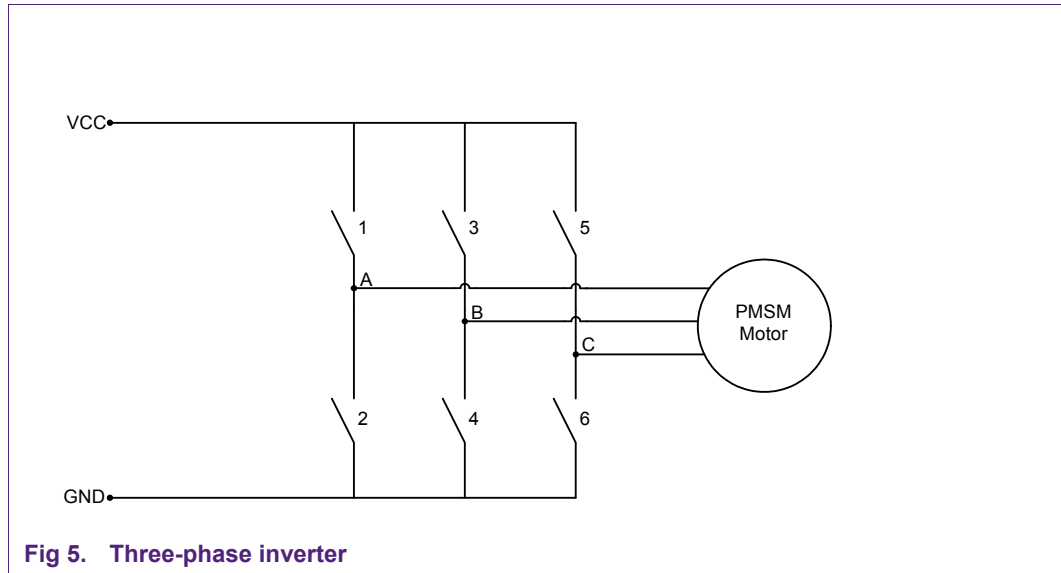
Inverse Park:

$$V_\alpha = V_d \cdot \cos \alpha - V_q \cdot \sin \alpha \tag{7}$$

$$V_\beta = V_d \cdot \sin \alpha + V_q \cdot \cos \alpha \tag{8}$$

2.3 SVPWM

Space Vector Pulse Width Modulation is a technique to generate three-phase PWM signals. The principle of a three-phase inverter is shown in [Fig 5](#).



Each phase of the three-inverter outputs can be driven high or low. In every branch there is always one switch open and one switch closed. If both switches are closed, a short-circuit situation is created. This means that there are eight possibilities depending on the switches that are turned on. The two states where all three outputs are connected to the positive or the negative supply are called zero states or zero vectors. In that case there is no potential difference between any of the phases.

Table 2. Switching states

| | Space vector | Switching state | On' switches |
|---------------|--------------|-----------------|--------------|
| Zero vector | V7 | [111] | 1.3.5 |
| | V0 | [000] | 2.4.6 |
| Active vector | V1 | [001] | 2.4.5 |
| | V2 | [010] | 2.3.6 |
| | V3 | [011] | 2.3.5 |
| | V4 | [100] | 1.4.6 |
| | V5 | [101] | 1.4.5 |
| | V6 | [110] | 1.3.6 |

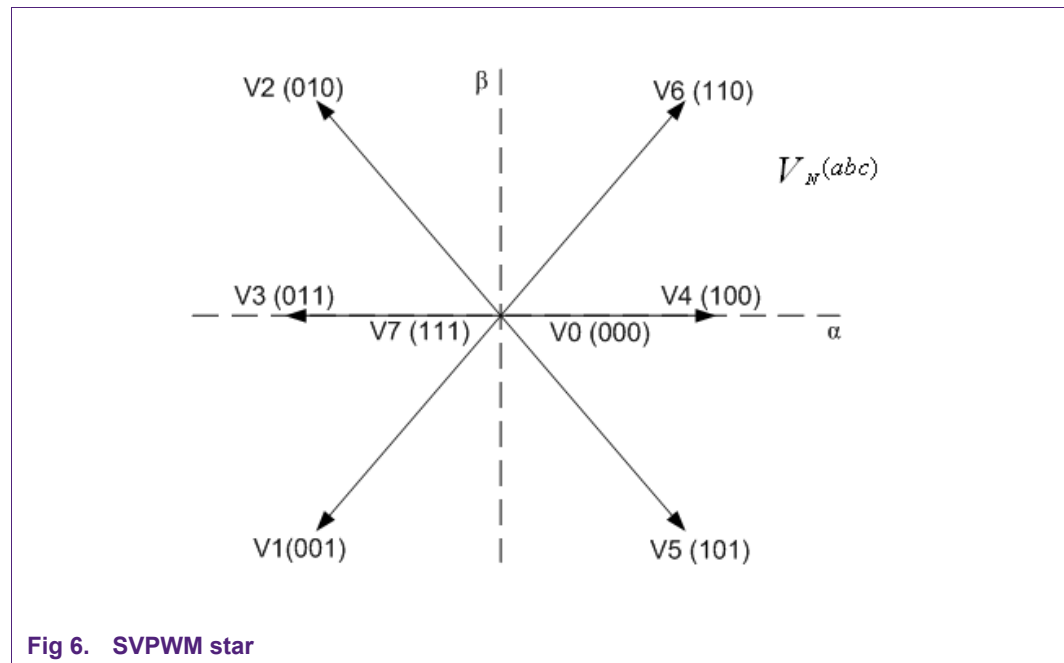


Fig 6. SVPWM star

Fig 6 shows how the active vectors divide the plan into six sectors. Depending on the sector that the voltage reference is in, two adjacent vectors are chosen. The binary representations of two adjacent basic vectors differ in only one bit. The vectors are time weighted in a sample period T to produce the desired output voltage.

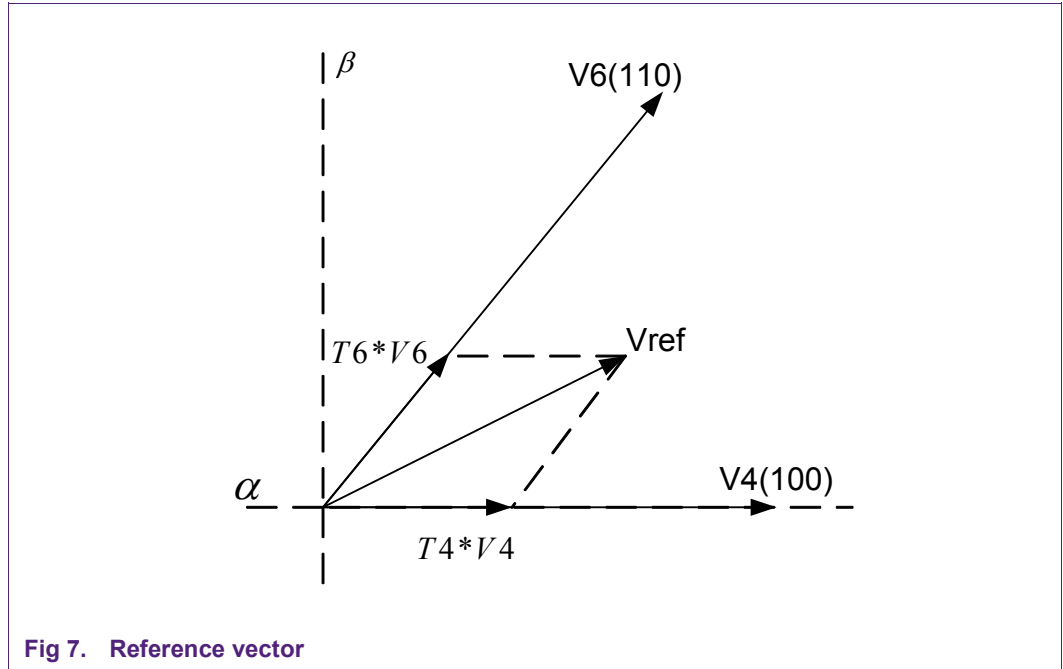


Fig 7. Reference vector

The length of the vectors T4 and T6 represent the amount of the time V4 and V6 are active and vary depending on the angle and amplitude of the voltage reference vector. In other words, T4 represents the on-time of V4, which activates switches 1, 4 and 6 as can be seen from Table 2. Dividing the actual time t4 by T produces a normalized time vector T4. The on-time of the vectors T4 and T6 can be calculated with the sine rule:

$$T4 = V_{ref} \cdot \left(\cos(\alpha) - \frac{1}{3}\sqrt{3} \cdot \sin(\alpha) \right) \tag{9}$$

$$T6 = 2 \cdot V_{ref} \cdot \frac{1}{\sqrt{3}} \cdot \sin(\alpha) \tag{10}$$

When V_{ref} is smaller than V4, which is typically maximum $\frac{2}{3} V_{dc}$, one of the zero vectors (V0 or V7) have to be used to produce no torque for a period equal to:

$$T0 = 1 - T4 - T6 \tag{11}$$

Different strategies are possible in sequencing V4, V6 and one of the zero vectors V0 or V7. The strategy that induces the least harmonic distortions on the output line voltage uses a center aligned seven-segment technique. The sequence V0-V4-V6-V7 is used in the first half period, and V7-V6-V4-V0 in the second half period. The sequences are symmetrical. An example period with seven segments is shown in Fig 9. In the middle of the pattern, zero-vector V7(111) is selected instead of zero-vector V0(000). To go from V6 to V7 requires only one of three branches of the three-phase inverter to be switched. This minimizes the number of switching actions.

2.4 Duty cycle calculation

The next step in SVPWM control is to calculate the actual duty cycle value for each phase. First it is important to determine which sector is currently active by evaluating the rotor angle. For calculation, use only the adjacent vectors in the given sector.

Lets assume for example that $V_{ref} = 10V$, $V_{dc} = 12V$ and the rotor angle equals 20 degrees. This angle refers to the first sector of the SVPWM hexagon, therefore $V_4(100)$, $V_6(110)$, $V_0(000)$ and $V_7(111)$ are used for calculation.

$$T_4 = \frac{10V}{12V} \cdot \left(\cos(20) - \frac{1}{3}\sqrt{3} \cdot \sin(20) \right) \cdot 100\% = 62\% \tag{12}$$

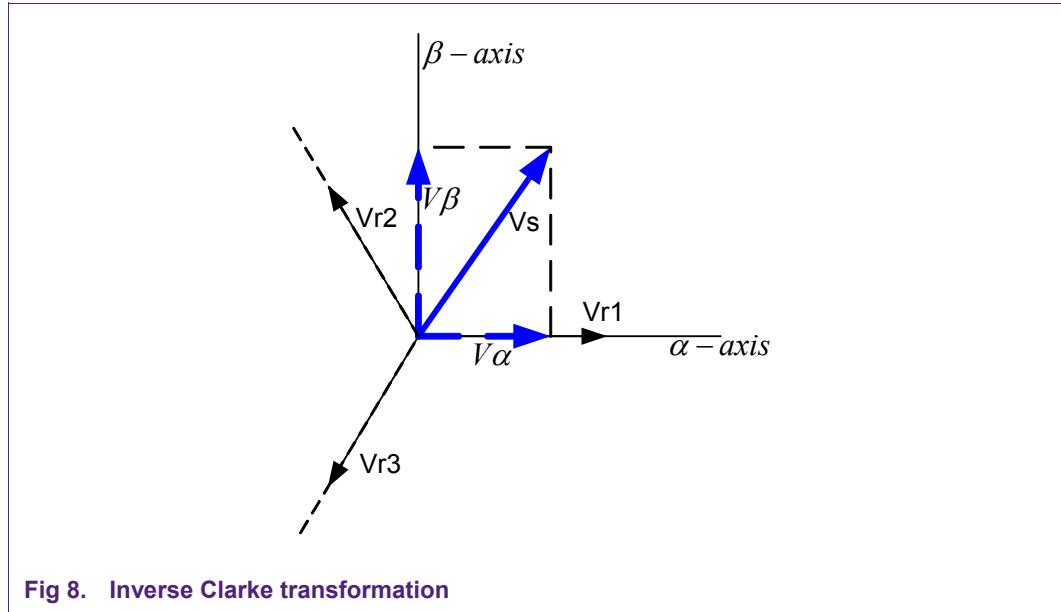
$$T_6 = 2 \cdot \frac{10V}{12V} \cdot \frac{1}{\sqrt{3}} \cdot \sin(20) \cdot 100\% = 33\% \tag{13}$$

$$T_{0,7} = 100\% - T_4 - T_6 = 5\% \tag{14}$$

The duty cycle equals the sum of the corresponding components of the adjacent vectors multiplied by their 'on-time'. Remember that a seven-segment SVPWM pattern is chosen where half the time of the zero-vectors V_0 is used and V_7 for the other half. When V_0 is used, none of the switches are active, so the contributing value to the PWM will always be zero and therefore can be neglected.

| | | |
|-----------------------------------|-------------------------------|---|
| PWM = V_4 component * 'on-time' | + V_6 component * 'on-time' | + V_7 component * $\frac{1}{2}$ 'on-time' |
| PWM1 = $1 * 62\%$ | + $1 * 33\%$ | + $1 * \frac{1}{2} * 5\% = 97,5\%$ |
| PWM2 = $0 * 62\%$ | + $1 * 33\%$ | + $1 * \frac{1}{2} * 5\% = 35,5\%$ |
| PWM3 = $0 * 62\%$ | + $0 * 33\%$ | + $1 * \frac{1}{2} * 5\% = 2,5\%$ |

This calculation requires the angle and the length of the voltage reference vector. The output of the PI regulation however consists off the α and β component of the voltage vector. A smarter approach of calculating the PWM values is to transform the two-phase voltage vector into a three phase vector V_1 , V_2 and V_3 using a modified inverse Clarke transformation.



$$V_{r1} = V_{\beta} \tag{15}$$

$$V_{r2} = -\frac{1}{2}V_{\beta} + \frac{1}{2}\sqrt{3} \cdot V_{\alpha} \tag{16}$$

$$V_{r3} = -\frac{1}{2}V_{\beta} - \frac{1}{2}\sqrt{3} \cdot V_{\alpha} \tag{17}$$

By reversing V_{α} and V_{β} a reference axis is created that is shifted thirty degrees from the SVPWM star. As a result two of the three phases Vr1, Vr2 and Vr3 are symmetrically bound to the SVPWM star, and one axis is exactly opposite. The values on the two bound axes are equal to the time vectors T4 and T6.

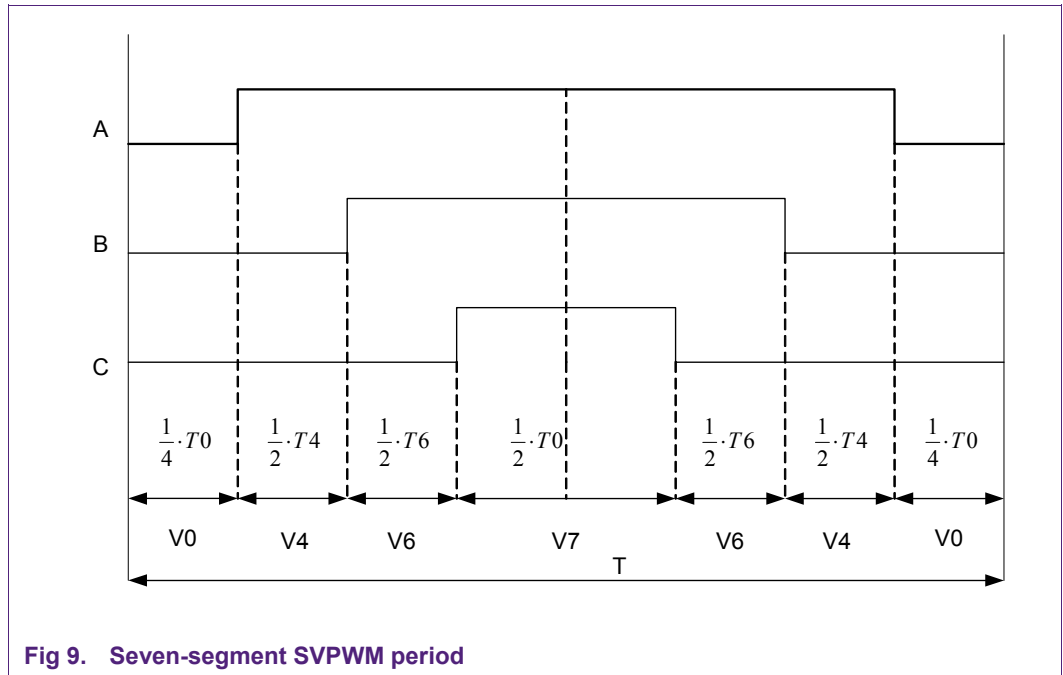


Fig 9. Seven-segment SVPWM period

After normalizing the voltage vectors the duty cycle can then be calculated. A full period T is equal to $T = T_0 + T_4 + T_6$. From [Fig 9](#) the duty cycle of phase C is equal to:

$$C = \frac{1}{2}T_0 \tag{18}$$

Substitution for $T_0 = 1 - T_4 - T_6$ leads to:

$$C = \frac{1}{2}(1 - T_4 - T_6) \tag{19}$$

$$B = C + T_6 \tag{20}$$

$$A = B + T_4 \tag{21}$$

For calculation of the real duty cycle, substitute values T_4 and T_6 for the two voltage reference vectors that correspond with the bound axes of that sector. Therefore, in each sector, the duty cycle calculation is done by different combination of vectors for the different phases. The easiest way to implement this in software is to use a state machine depending on the sign of the voltage vectors.

2.5 Current vector reconstruction

Though the current of the phases can be measured by using a shunt for each phase, a single DC-link shunt is used for current sensing. The current of a phase is measured when only that phase is active. The timing of the sample moment is critical because the sample window only lasts until the rising edge of the next phase. In some cases SVPWM produces a duty cycle value for phase A and B that are of similar values. In this case separated phases cannot be measured because both phases share the same rising and falling edges.

It is possible to shift phases A and B while maintaining their duty cycle values. When the time difference between two rising edges is smaller than the FET stabilizing time plus the sample time (t_{sample}), the phases need to be shifted apart. When the duty cycles of all three phases are equal, all phases need to be shifted. In order to keep the shifting time to a minimum, a high speed ADC with a narrow sample window is needed.

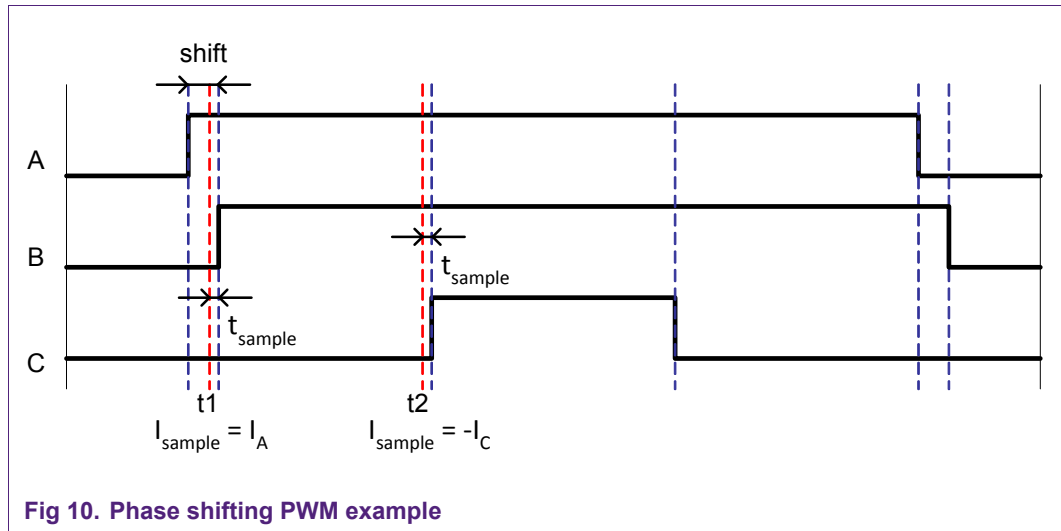


Fig 10. Phase shifting PWM example

In the example of Fig 10 the first sample point (t_1) equals the rising edge of phase B minus the sample time (t_{sample}). The sampled value (I_{sample}) represents the current through phase A. The second sample point (t_2) equals the rising edge of phase C minus the sample time. This time sampled value represents the current through phases A and B, which equals minus C. Because all three windings are interconnected the sum of the currents through phases A, B and C equals zero.

$$I_a + I_b + I_c = 0 \tag{22}$$

This means that only two out of three phases have to be measured. The current of phase B can be calculated and is equal to $-I_A - I_C$.

2.6 FOC overview

Fig 11 shows the concept for speed control with FOC. The block schematic is divided in several subsystems.

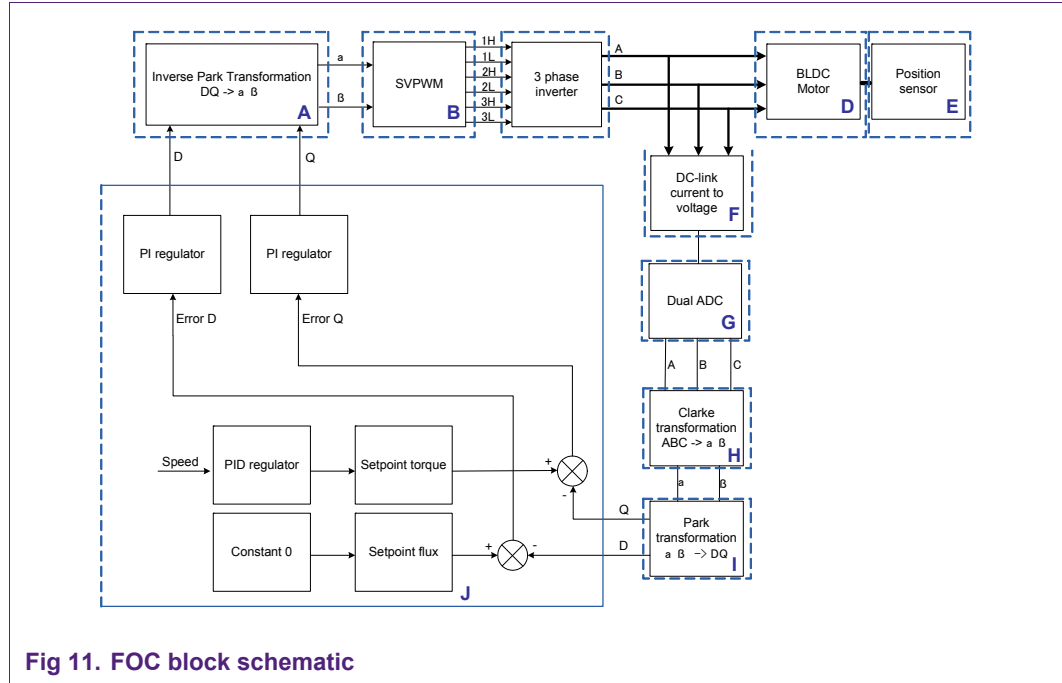


Fig 11. FOC block schematic

Table 3. Description subsystems

| Subsystem | Description | Function |
|-----------|---|--|
| A | Inverse park transformation | Convert V_q and V_d setpoint to the static reference frame |
| B | Space vector pulse width modulation (SVPWM) | Generate PWM signals from SVPWM start for inverter according to Voltage reference vector |
| C | 3-phase inverter | Apply PWM signals to the BLDC motor |
| D | Brushless motor (PMSM) | Used motor |
| E | Position sensor | Obtain rotor position. Needed for FOC transformations and speed calculation. |
| F | DC-link current | Dual ADC for time independent DC-link current measurements |
| G | Current vector reconstruction | Reconstruction of the current vector of the different phases. |
| H | Clarke transformation | Transformation from a three-phase to a two-phase system. |
| I | Park transformation | Transformation to a dynamic reference frame for time independent PI regulators. |
| J | PI regulation | Correct error between measured and reference user inputs. |

3. Sensorless FOC

3.1 Back-EMF principle

A brushless EC motor consists of stator coils and a permanent magnet rotor. The permanent magnet moving past the stator coils induces an electrical potential called Back Electro Motive Force (BEMF). In a trapezoidal control, the back-EMF can be measured by sampling the voltage on a floating phase. The zero crossing point can then be detected and the position of the rotor can be estimated. With this implementation of estimation of the rotor angle a sensor can be discarded.

Measurement of the back-EMF in combination with FOC however is not possible. With FOC all phases are commutated and no phase is left floating to be measured for back-EMF.

Still sensorless operation with FOC is possible. There are different approaches for estimating the rotor position of a PMSM motor. The approach chosen in this application note is to estimate the back-EMF with a current observer with a Slide Mode Controller (SMC) and subsequently estimating the rotor angle. The principle of a SMC is explained in the next paragraph.

In [Fig 12](#) a basic stator model of a DC-motor is shown, represented by winding resistance, winding inductance and back-EMF.

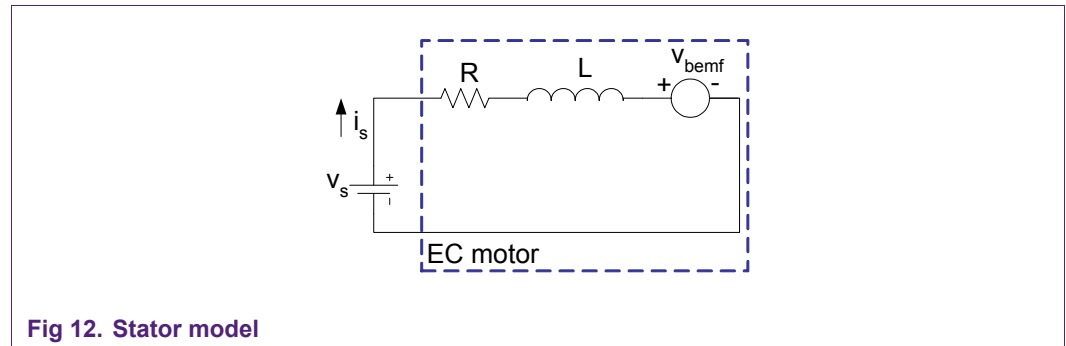


Fig 12. Stator model

The back-EMF is independent of the energy supplied to the motor. It is directly proportional to the rotation speed, the rotor flux and the number of turns in the corresponding winding. In one turn of the winding, the back-EMF equation is:

$$v_{bemf} = \frac{-d\Phi}{dt} \tag{23}$$

where $d\Phi$ is the rotor flux. E will be at its maximum when the variation of the flux is at maximum. This happens when the rotor passes from a North to a South Pole. This means that the back-EMF is at maximum when the rotor flux is perpendicular to the phase.

From the motor model, the input voltage can be obtained by the following equation:

$$v_s = R \cdot i_s + L \cdot \frac{d}{dt} i_s + v_{bemf} \tag{24}$$

where:

i_s = Motor Current Vector (A)

v_s = Input Voltage Vector (V)

v_{bemf} = Back-EMF Vector (V)

R = Winding Resistance (ohm)

L = Winding Inductance (H)

The subscript s represents a two-dimensional vector on the α and β axes.

The motor current is obtained by solving for i_s :

$$\frac{d}{dt} i_s = \left(-\frac{R}{L} \right) i_s + \frac{1}{L} (v_s - v_{bemf}) \quad (25)$$

The goal of this formula is to calculate a new estimated current based on an estimated back-EMF voltage. In the digital model $\frac{d}{dt} i_s$ is equivalent to the current change during one control period. This can be represented by the difference between the new estimated current (i_{est}) minus the previous current (i_s) divided by the period time (T). The equation now becomes:

$$\frac{i_{est} - i_s}{T} = \left(-\frac{R}{L} \right) i_s + \frac{1}{L} (v_s - v_{bemf}) \quad (26)$$

Solving for i_{est} :

$$i_{est} = \left(1 - T \cdot \frac{R}{L} \right) i_s + \frac{T}{L} (v_s - v_{bemf}) \quad (27)$$

R and L are static parameters that are dependent on the motor hardware. R and L can be measured and represent half the value measured phase-to-phase with a RCL- or multimeter. T is the control period, which is also known. Substitution of the constant parameter R, L and T yields:

$$F = \left(1 - T \cdot \frac{R}{L} \right) \quad (28)$$

$$G = \frac{T}{L} \quad (29)$$

$$i_{est} = F \cdot i_s + G \cdot (v_s - v_{bemf}) \quad (30)$$

3.2 Slide Mode Controller

As described in the previous paragraph the basic principle of sensorless FOC is estimating the rotor angle Φ and speed ω needed for FOC commutation by estimating the Back-EMF based on measured currents and calculated voltages. The principle of calculating the current rotor angle Φ is based on creating a virtual model that equals the physical model. An overview of the control is shown in Fig 13.

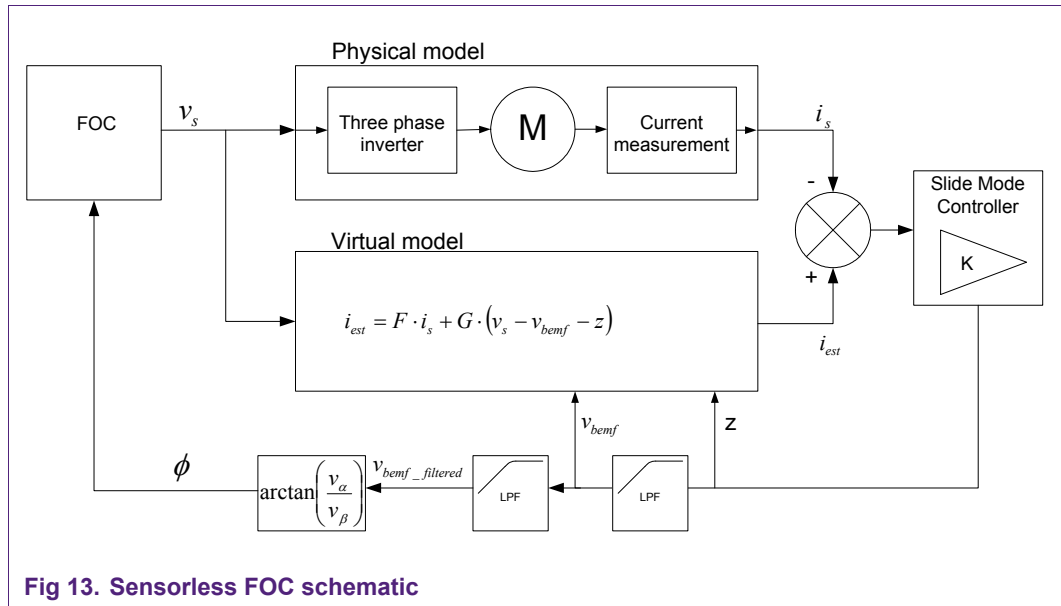


Fig 13. Sensorless FOC schematic

Both the physical and the virtual motor share the same input V_s . The estimated current output of the virtual model should match the physical model. Error in the virtual model is corrected by introducing a correction factor z . This factor is included in the calculation of the estimated current and minimizes the differences between the physical and the virtual model. The factor z is controlled by a slide mode controller (SMC), which multiplies the errors of I_α and I_β with a gain K . The slide mode controller has a linear amplification gain K within defined bounds to a certain maximum estimated current error. If the error exceeds the boundary, z is clipped.

Because the only input for the back-EMF in the virtual motor is the correction factor z , this factor z represents the actual value of the back-EMF when filtered with a low pass filter. A dynamic filter frequency is used with a cutoff frequency matching frequency of the drive currents and voltages in the motor, which equals the speed.

$$f_{cutoff} = 2\pi \cdot \frac{RPM \cdot polepairs}{60} \tag{31}$$

$$\omega_{cutoff} = 2\pi \cdot f_{cutoff} \tag{32}$$

$$c_{filter} = T \cdot \omega_{cutoff} = T \cdot 2\pi \cdot \frac{RPM \cdot polepairs}{60} \tag{33}$$

In software the motor speed ω is acquired by accumulating the calculated angle from the back-EMF voltages over a period of time t_{acc} .

$$\omega = \frac{\alpha_{acc}}{t_{acc}} \tag{34}$$

$$RPM = \frac{\alpha_{acc} \cdot 60}{2\pi \cdot t_{acc} \cdot polepairs} \tag{35}$$

This means that:

$$c_{filter} = \alpha_{acc} \cdot \frac{T}{t_{acc}} \tag{36}$$

Since the input frequency is equal to the cutoff frequency, the phase delay of the filter is -45° . The same filter coefficient is used again for input signal of the calculation of the rotor angle α . This is done for creating a smoother output signal. The total phase delay then becomes -90° .

The rotor angle (α) is calculated by the arctangent of the filtered back EMF voltages that are 90° out of phase.

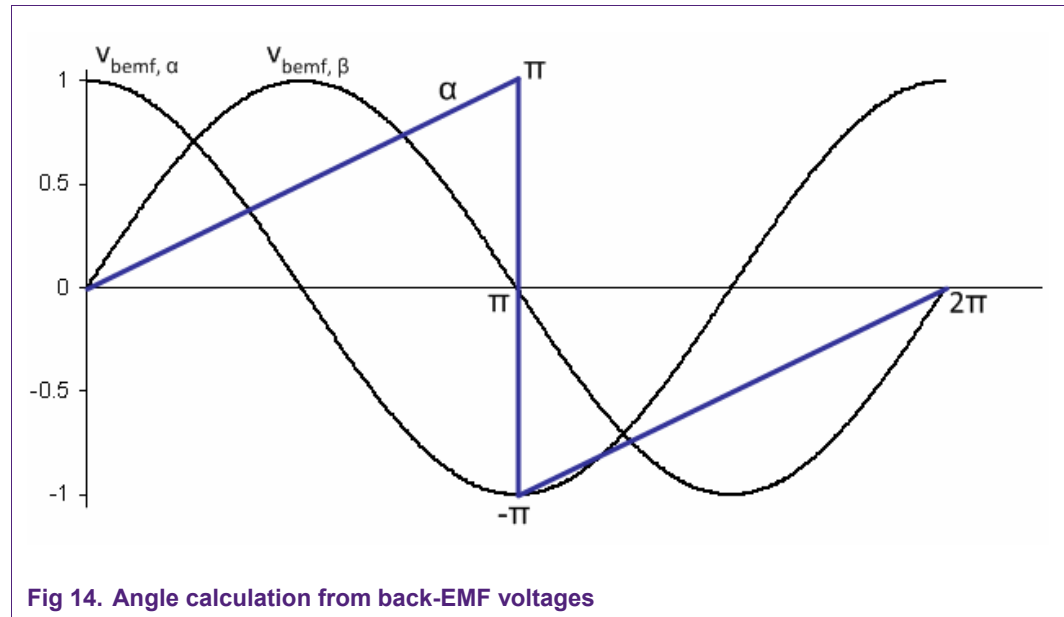


Fig 14. Angle calculation from back-EMF voltages

$$\alpha = \arctan\left(\frac{v_{bemf\alpha}}{v_{bemf\beta}}\right) \tag{37}$$

3.3 Phase compensation

The two first order filters on the theta calculation create a phase delay that has to be compensated in the calculation of the rotor angle. The amount of compensation depends on the motor speed ω .

The arctangent output of the back-EMF voltages is multiplied by a gain K and added with a constant offset C. The gain and offset are values stored in a lookup table that depend on the motor speed. Calibration of the phase compensation is needed for any particular motor.

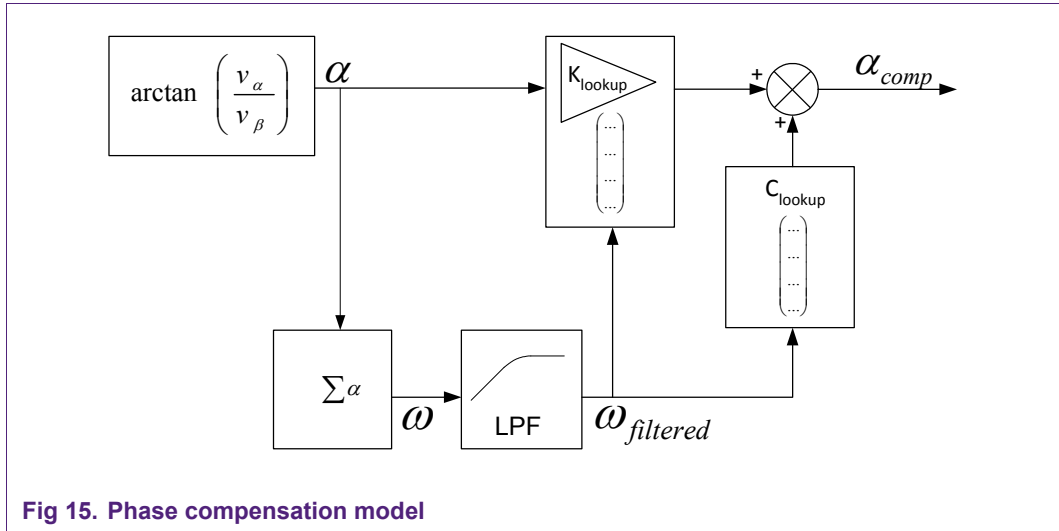


Fig 15. Phase compensation model

One way to acquire the calibration values is to compare the uncompensated angles from the virtual motor to the angles read from a QEI. The error of the uncompensated angles from the virtual motor can be plotted against the speed. Calibration values can then be extracted from the plot. When a QEI is absent, calibration values have to be determined experimentally.

4. Hard- and software

4.1 FOC Demoboard

The FOC demoboard is designed with a LPC2900 microcontroller for its specific features and peripherals, which are highlighted in the next paragraphs.

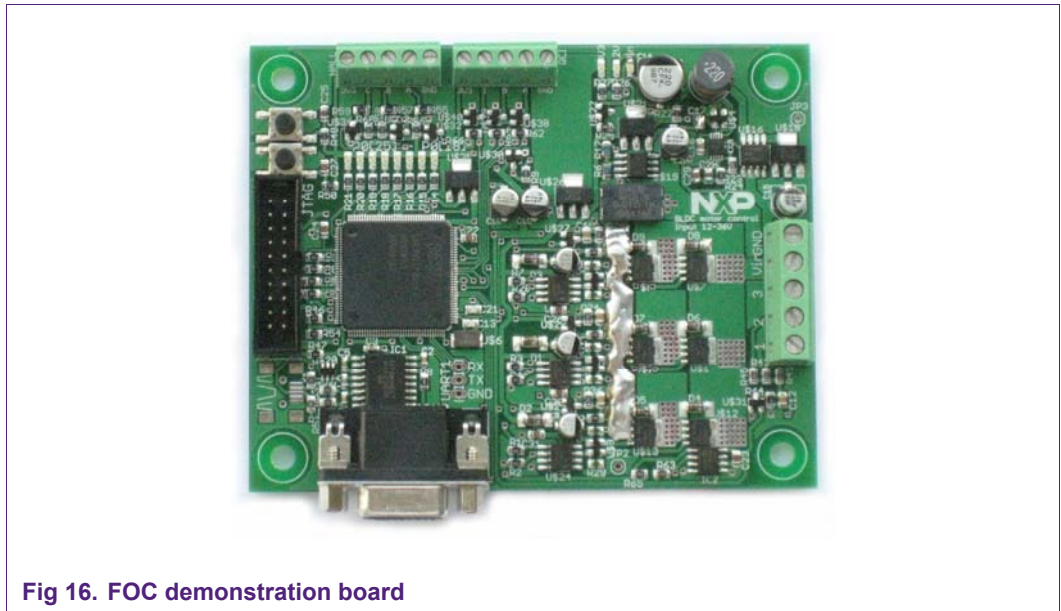


Fig 16. FOC demonstration board

4.2 Three phase inverter

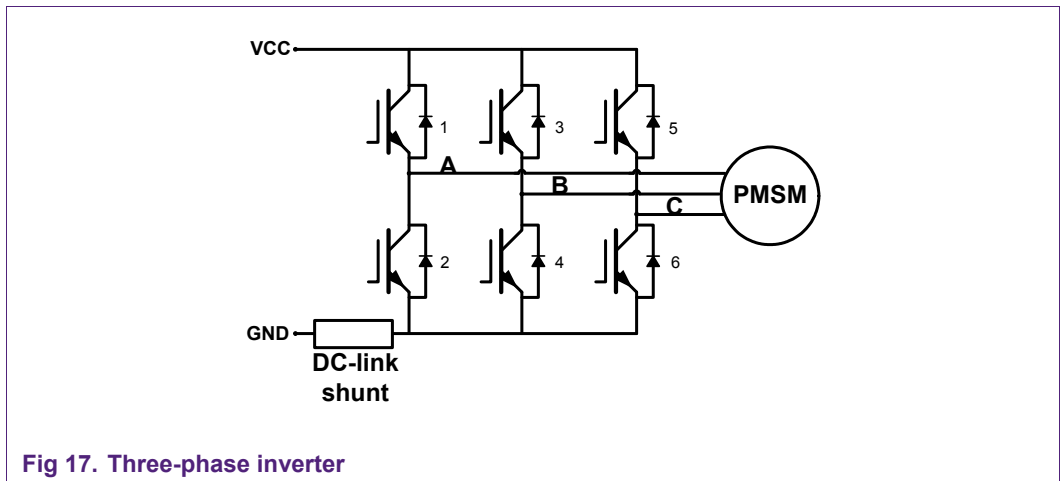


Fig 17. Three-phase inverter

In [Fig 17](#) a basic three-phase inverter is shown. The inverter consists of three single-phase inverter switches each connected to one of the three windings. The electronic switches consist of N-channel PSMN2R6-40YS MOSFET's with a voltage rating of 40V and a very low resistance ($R_{DS(ON)}$) of 2.8 m Ω . The lower the resistance, the lower the power loss when current is flowing through the MOSFET's.

Alternatives depend on the desired operating voltage of the motor. The NXP Trench 6 MOSFET series cover a range from 25V to 80V with a low $R_{DS(ON)}$, a low gate charge and a Power-SO8 footprint.

The output of the LPC2900 is amplified by bridge driver IC's with a bootstrap to raise the voltage level on the gates of the MOSFET's.

4.3 DC-link current measurement

Two ADC's are used for mutually independent sample times of the DC-link current. The output of the current sensing circuit is fed into ADC1 and ADC2.

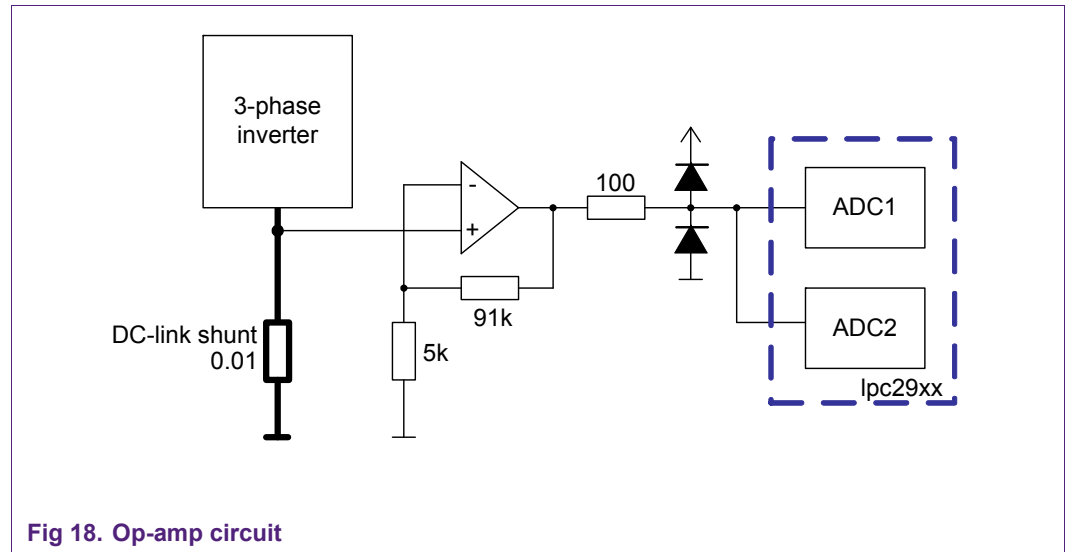


Fig 18. Op-amp circuit

The sink of the three-phase inverter is fed through a 0.01Ω 3-Watt shunt resistor. A high-speed precision op-amp is used (AD823 16MHz) to amplify the voltage over the shunt resistor. Because of the limited time frame for the ADC's to take a sample of the voltage over the shunt an op-amp is needed with a high slew rate and fast settling time.

The gain off the op-amp circuit on the demo board is:

$$G = \frac{91k}{5k} + 1 = 19.2 \tag{38}$$

The maximum analog input voltage of the ADC is 3.3V. Dividing the gain by a 19.2 results in a maximum voltage of 0.172 V across the shunt. The maximum measured current is therefore 17.2 Amps. The maximum dissipated power in the shunt is 0.172 V * 17.2 A = 3W. If a larger current draw is required the value of the shunt can be lowered.

4.4 LPC2900 MSCSS

The LPC2900 series features a Modulation and Sampling Control Subsystem that is able to synchronize ADC's and PWM blocks.

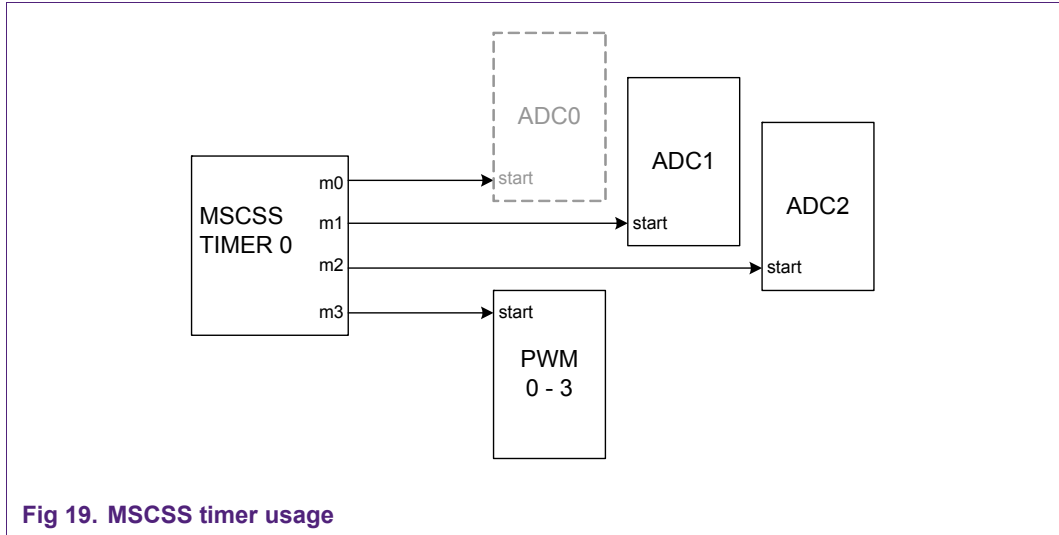


Fig 19. MSCSS timer usage

The mtimer0 runs at 20kHz. The value of match3 is 0, so the PWM is synchronized with the mtimer0. Because ADC0 is 5V, the 3.3V ADC's 1 & 2 are used instead. When the mtimer0 counter reaches the match1 value, ADC1 is started. ADC2 is triggered by match2. By using the mtimer0 the exact ADC sample points can be set. The ADC's are configured to 10bit sampling at 400 kHz. The ADC clock runs at 4.5 MHz. The signal is sampled in one clock cycle, which equals to 0.22 μs. After that it takes a number of clock cycles equal to the number of resolution bits to convert it to a digital value.

Full control of the rising and falling edges of the PWM signal is needed to allow time shifting of the PWM phases. The LPC2900 series provides a PWM block where the MTCHACT register defines the position of the rising edge (activate) while the MTCHDEACT register defines the falling edge (de-activate) of the waveform. [Fig 20](#) shows the basic functionality of the PWM modulator.

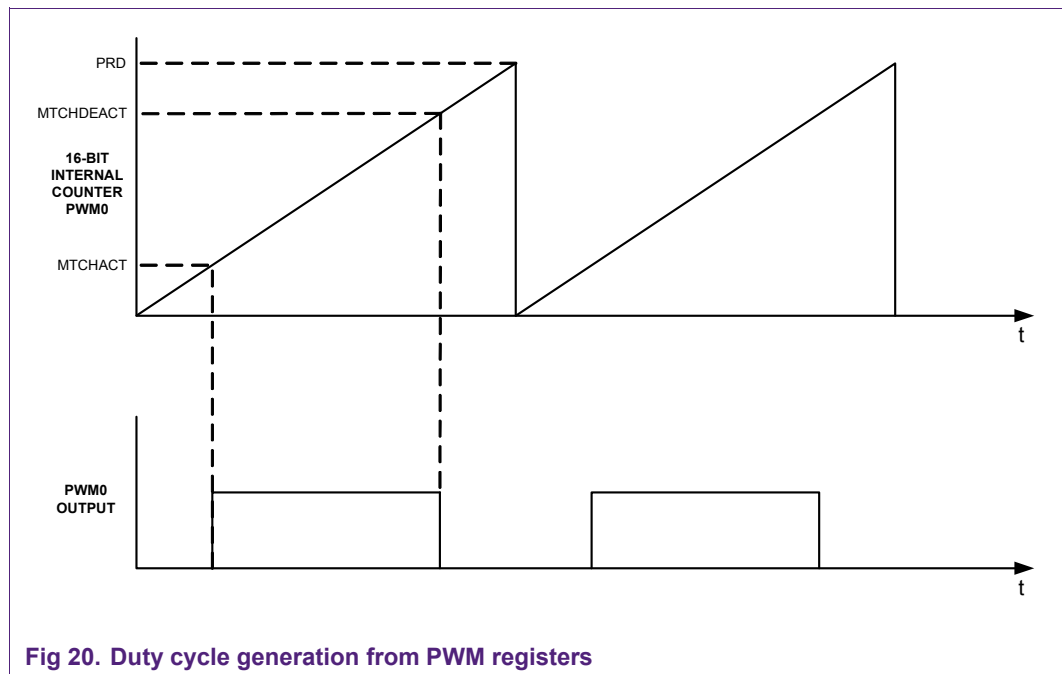


Fig 20. Duty cycle generation from PWM registers

The PWM output changes when the internal PWM counter matches the values defined in the related registers (MTCHACT and MTCHDEACT). Also a mechanism is provided to allow an atomic change of the PWM configuration without disturbing the currently generated PWM outputs. Therefore two sets are available for each register. The software uses one set while the other set - the shadow registers - is used by the PWM. The lpc29xx contains 4 PWM blocks with six PWM channels each. For the three-phase inverter control a single PWM block is used.

4.5 FOC demoboard additional features

Other features of the demoboard are:

- Quadrature Encoder Interface. Connection supported of a QEI with a power supply of 5 volts.
- Temperature reading. A NXP SE95 temperature sensor is placed next to one of the MOSFET's. This temperature reading IC is connected over I²C.
- Push button. A button with a pull-up to Vcc is connected to an external interrupt port.
- RS232 connection over UART0. The DMA controller is used to loop transmission of a structure containing all FOC variables. The loop is configured with a linked list. The advantage of using DMA is a zero processor load. It accesses memory and transmits all data fully autonomic.

4.6 Software

Basically the whole FOC system is an interrupt-based system. At the beginning of the program, initialization takes place in the following systems.

Table 4. Program initialization

| System | Description |
|------------------|---|
| GPIO | The LED GPIO's need to be configured for output |
| Timer | The timer is initialized for controlling the LED's |
| I ² C | I ² C is used for communicating with a NXP SE95 temperature sensor |
| FOC variables | Various FOC variables need to be initialized |
| UART | UART0 is configured for interrupt-based reception |
| DMA | DMA is used to transmit a structure of FOC variables over UART0 by using a linked list. |
| PWM | PWM is configured to trigger on MTIMER0's sync signal |
| QEI | The Quadrature Encoder Interface |
| ADC | ADC1 & 2 are configured to trigger on MTIMER0's sync signals |
| MTIMER | The MTIMER0 is used for triggering the PWM period and the ADC conversions |
| EXTINT | The pushbutton is configured to raise an external interrupt |

The basic structure of the program is built around the MTIMER that triggers the PWM and the dual ADC's. At the end of the second ADC conversion an interrupt is generated that initiates the FOC control loop.

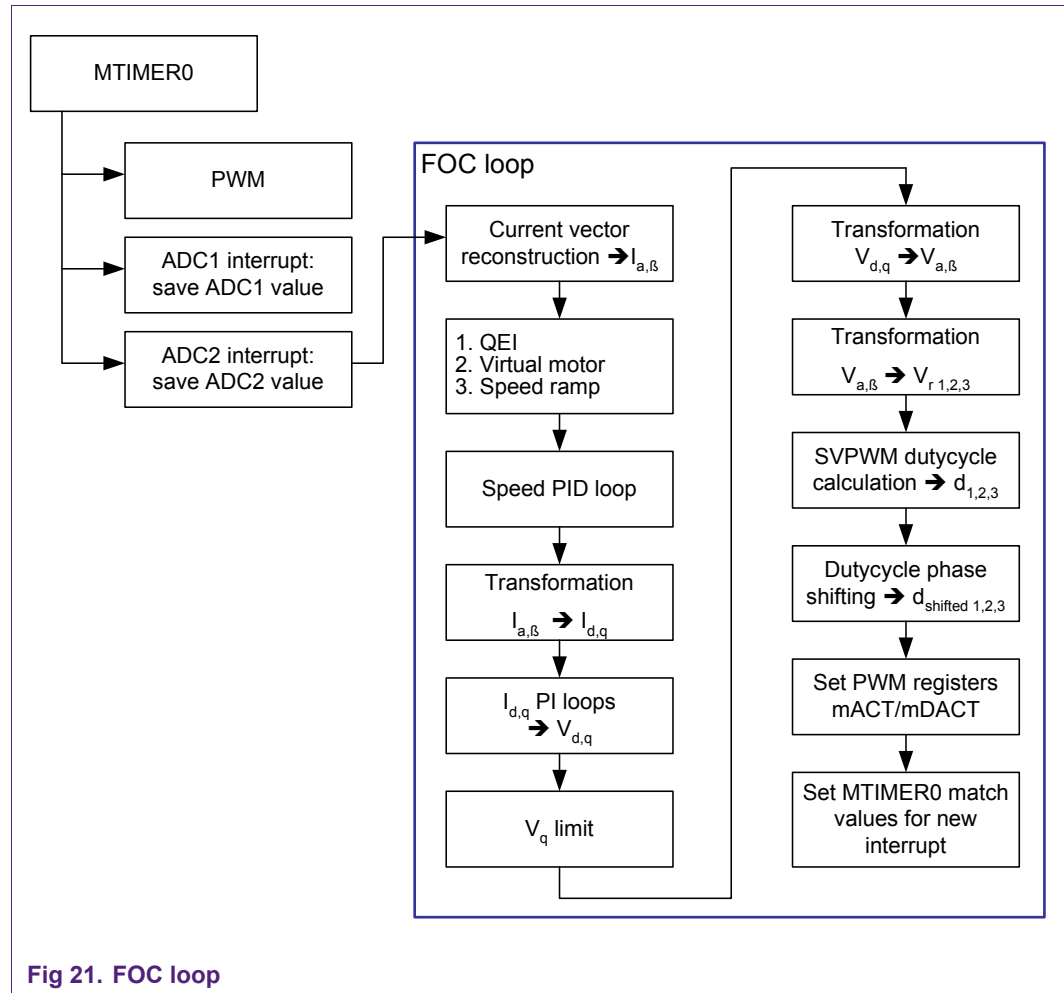


Fig 21. FOC loop

Three states are defined in software.

- a. QEI angle and speed reading
- b. Virtual motor angle and speed estimation
- c. Speed ramp

Two modes of operation are possible. In the first mode the QEI is used to read the actual angle and speed of the motor. In the second operation mode a speed ramp is used after initialization. When a certain defined minimum speed is reached, the system switches from to the 'Virtual motor' state where the angle and speed are estimated.

Fixed-point math calculations are used instead of floating point math to minimize the processor load. More information on fixed point is provided in Appendix II: Fixed point.

4.7 Dead time generation

For the three-phase inverter a dead-time interval is required to prevent a short circuit of a half-bridge (Fig 22) during a switching state change. If a switch of one inverter leg is turned on before the opposite switch blocks the bus voltage, then the entire bus is shorted. The MOSFET's have a delayed reaction to turn-off signals. After conducting, some time is needed to block the supply voltage.

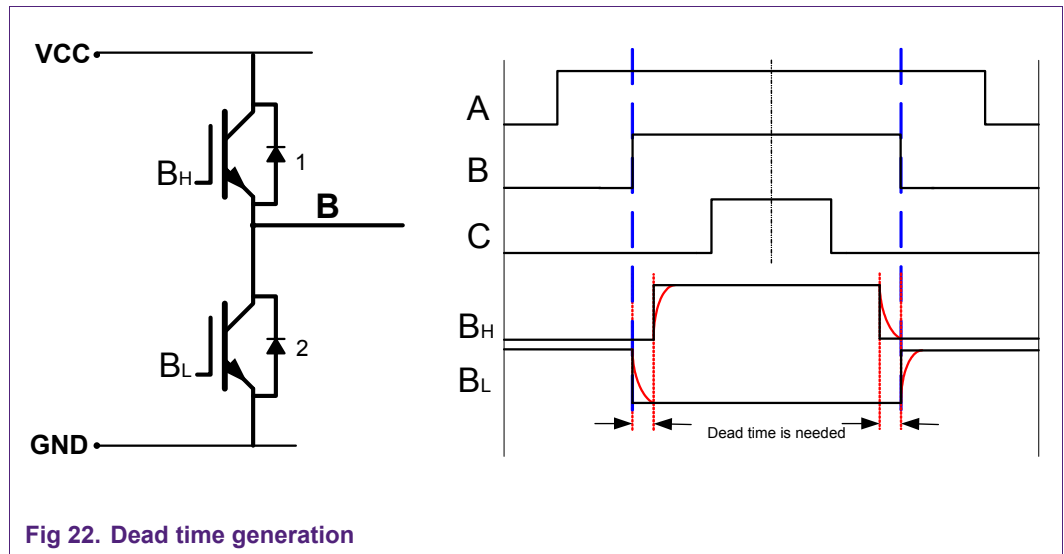


Fig 22. Dead time generation

If the low side switch is closed and the switching state is changed to high side (AH) a short circuit will occur when there is no dead time interval. A dead time interval must be introduced between the turn-off signal of the low side and the turn-on signal of the high side. Although the dead time is short it causes deviations from the desired inverter output voltage. Because of the dead time the duty cycles of the three phases will be slightly changed resulting into a less smooth line-to-line voltage.

4.8 Graphical user interface

The graphical user interface is capable of configuring different FOC parameters and displaying various signals. The purpose of the tool is to create a debug environment for developing FOC.

4.8.1 Q&D PI controllers tab

On the first tab the parameters of the Q and D PI controllers are displayed.

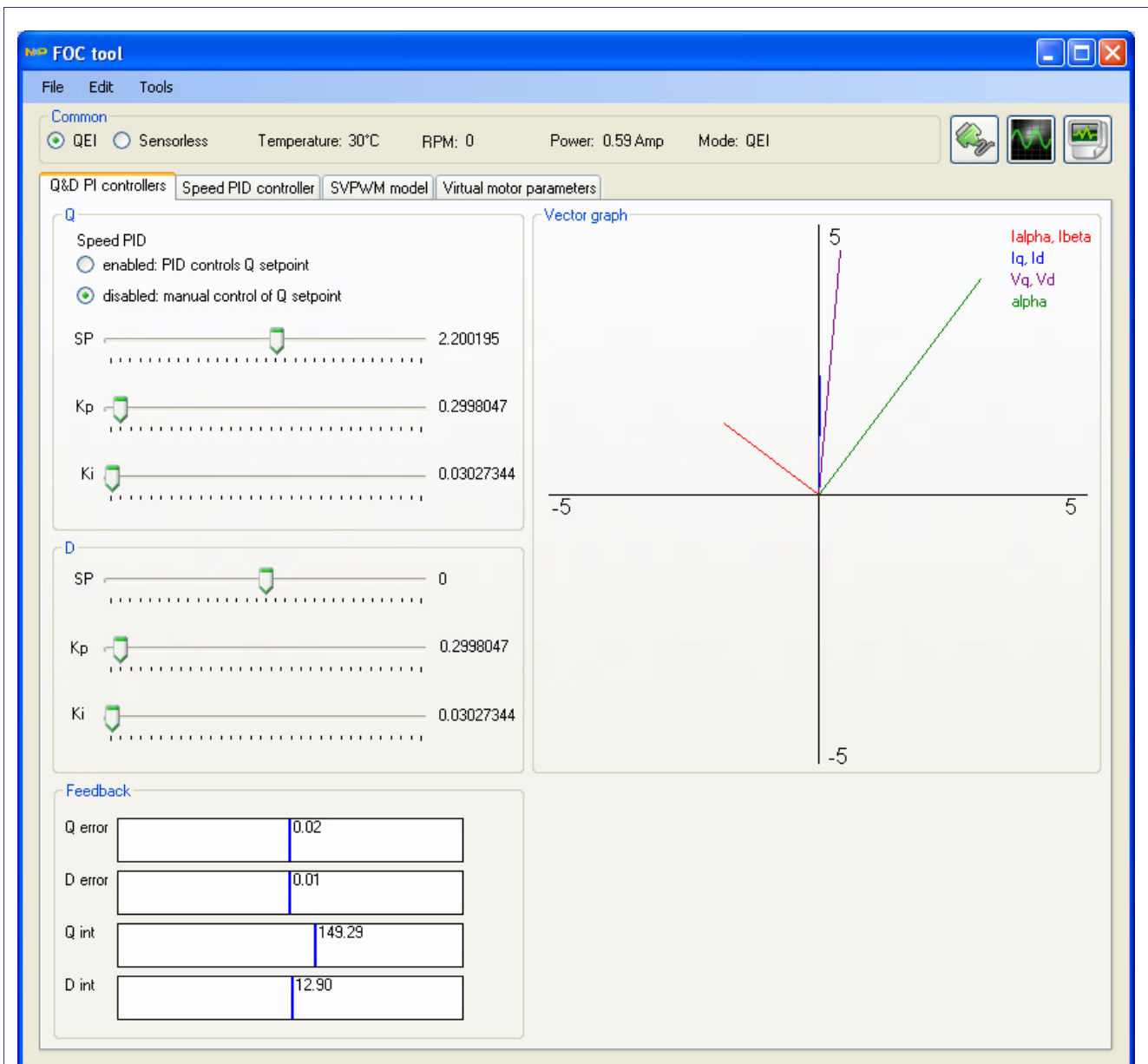


Fig 23. FOC tool: Q&D PI controllers tab

The setpoint for Q can be set manually by disabling the speed PID. When the speed PID is enabled, the speed controller takes over the setpoint value of Q. Using the sliders can modify the values of K_p and K_i for Q and D. The value is instantly transmitted to the demoboard when the COM connection is opened. The vector graph display's the current vectors $I_{\alpha-\beta}$, I_{q-d} and V_{q-d} . A green vector visualizes the rotor angle. The red current vector $I_{\alpha-\beta}$ is controlled perpendicular to the rotor angle by the magnitude and angle of the purple Voltage vector.

There is a possibility to instantly switch between QEI and sensorless operation. Next to the mode switching buttons, the most common variables are displayed like temperature, RPM, power and the current operation mode.

Next to the common group there are three buttons available:



Opens the COM port. Settings can be changed under menu edit → COM settings.



When the COM is opened, the button view changes to 'disconnect'. This closes the COM port.



Opens a new scope window. The number of scopes is unlimited. This feature is also available under menu Tools → Add scope. See section 4.8.6



Opens the datalogger window. This feature is also available under menu Tools → Datalogger. See section 4.8.7

4.8.2 Speed PID controller tab

On the second Speed PID controller tab, the parameters of the speed PID controller can be configured.

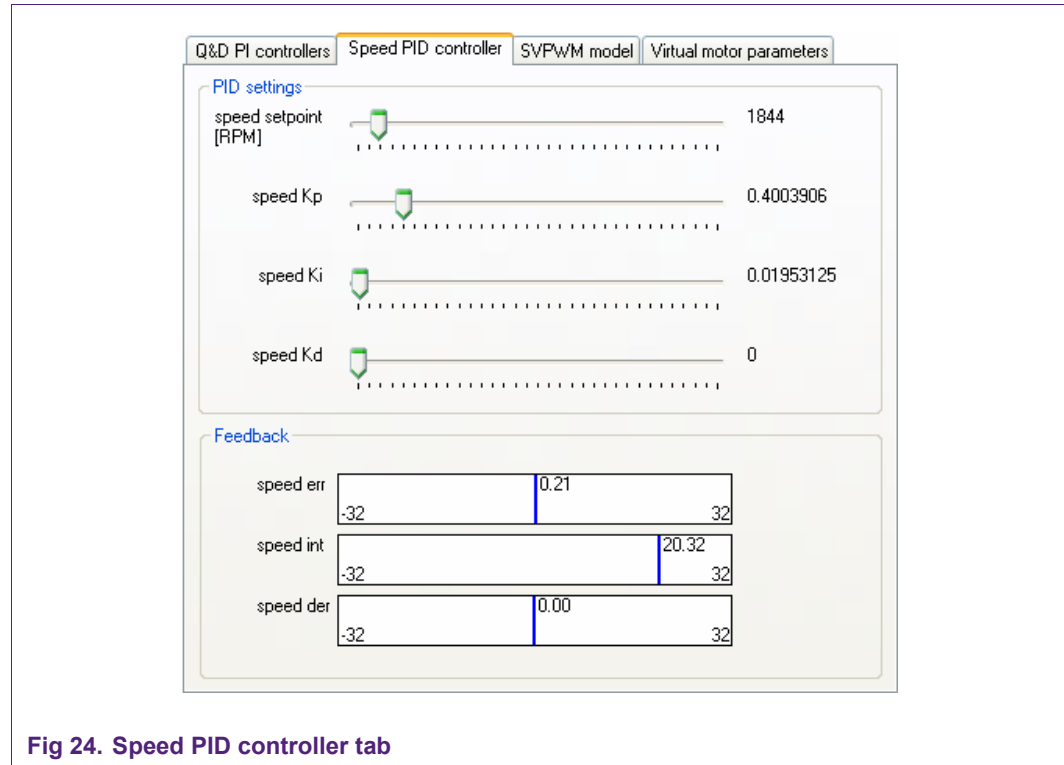


Fig 24. Speed PID controller tab

4.8.3 SVPWM model tab

On the SVPWM model tab, a SVPWM graph is displayed. Clicking in the SVPWM area can alter the vector length. By default the angle of the model is synchronized with the angle received from the demonstration board. When synchronization is deselected, the model can rotate automatically at a fixed speed by selecting auto rotate. There is also a possibility to transmit the PWM values generated by the model to the development board. Precaution is needed when transmitting high duty cycle values, which can cause a large current draw. Use of a current limited power supply is recommended.

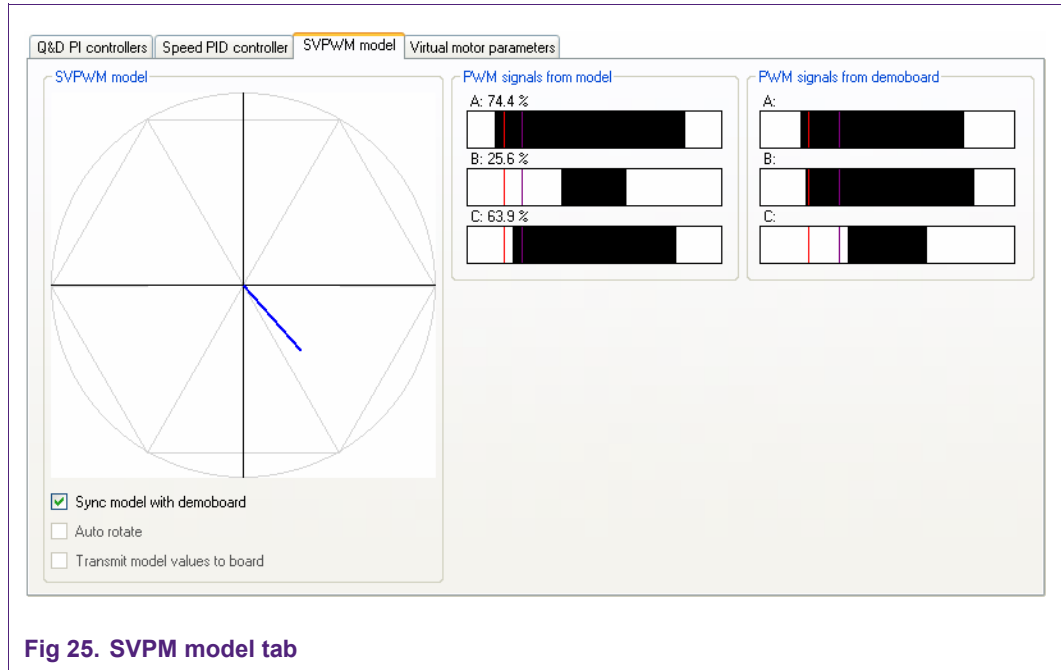


Fig 25. SVPWM model tab

4.8.4 Virtual motor parameters tab

On the virtual motor parameters tab, the motor specific settings can be configured.

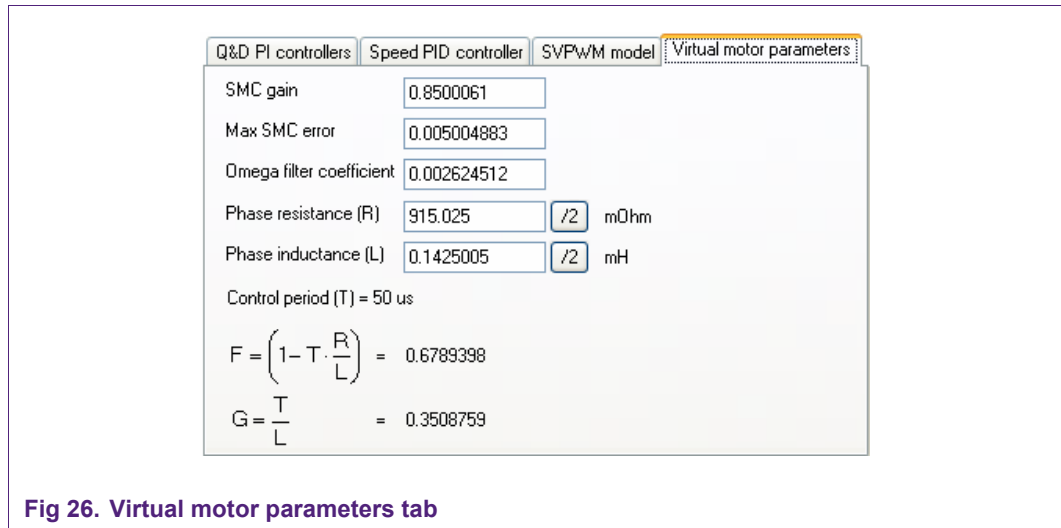


Fig 26. Virtual motor parameters tab

4.8.5 Open and save

Under menu file the options are given to open or save motor parameters. All the PI(D) controller values and the parameters under the virtual motor tab can be saved or loaded to a XML motor data file.

4.8.6 Scope window

A scope window can display variables that are constantly transmitted by the demoboard. A second channel is available by clicking the Channel 2 tab. By default it is set to <no signal>. The range of the output view is configurable by manually entering the maximum and minimum value. Auto ranging is also possible.

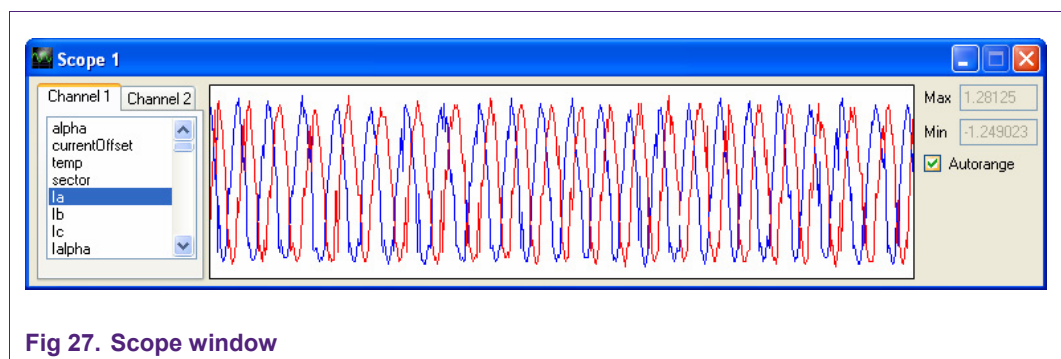


Fig 27. Scope window

4.8.7 Datalogger

To export the received signals to a text file and do further analysis in a spreadsheet program, a datalogger is available. Adding signal blocks and defining a column separator character can configure the output.

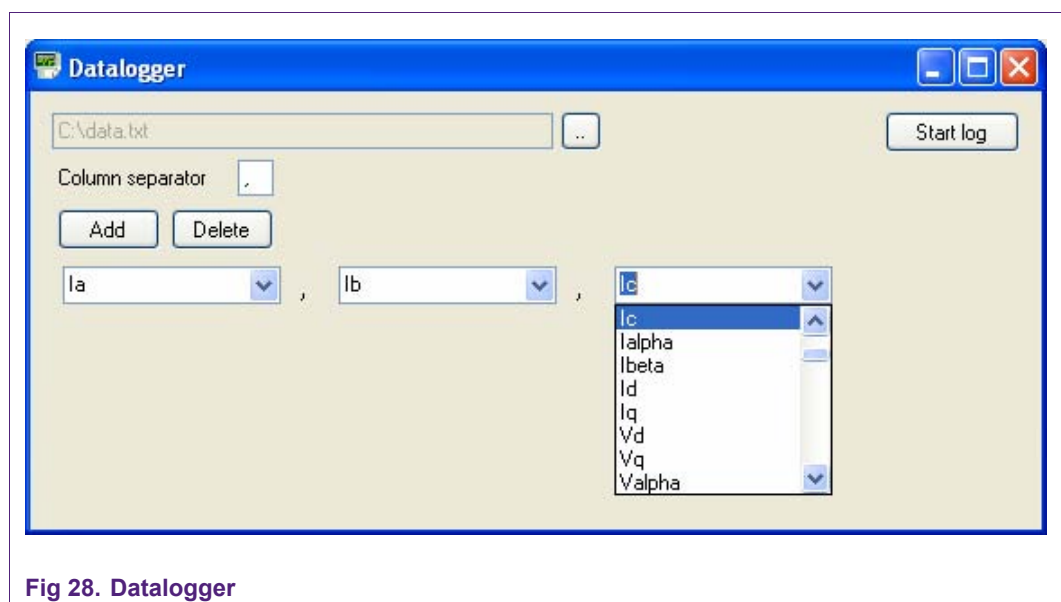
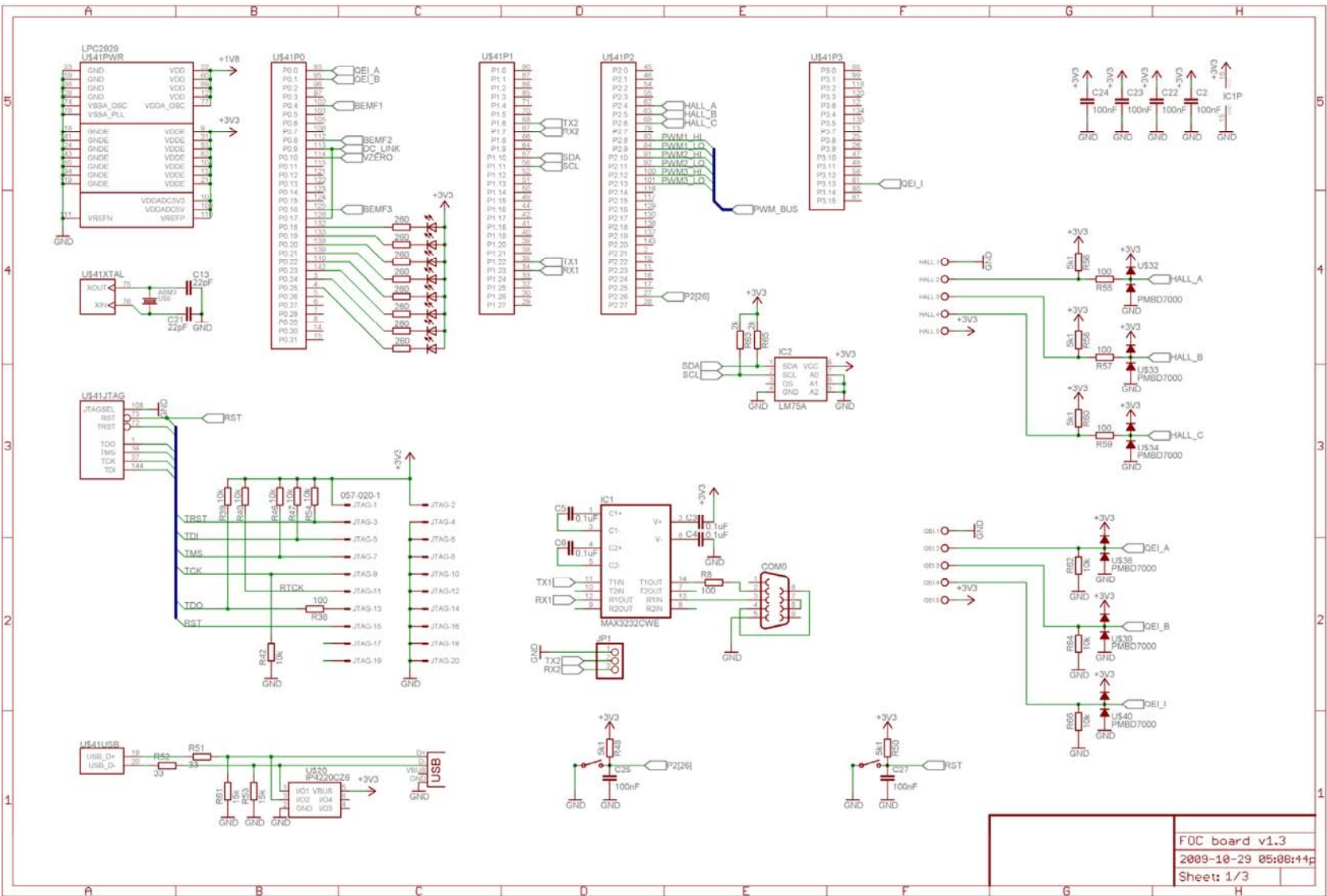
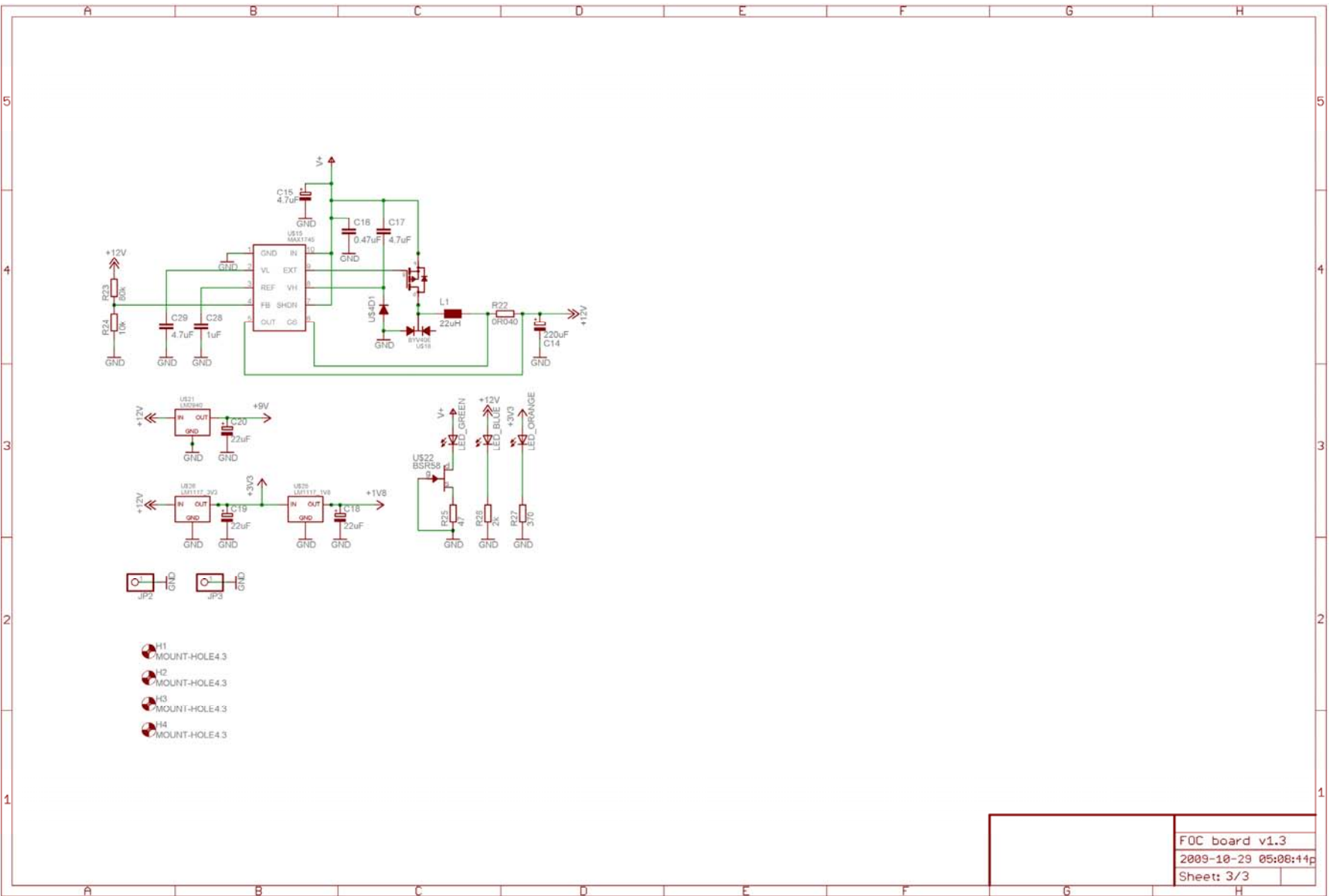


Fig 28. Datalogger

5. Appendix I: Hardware schematics



FOC board v1.3
2009-10-29 05:08:44p
Sheet: 1/3

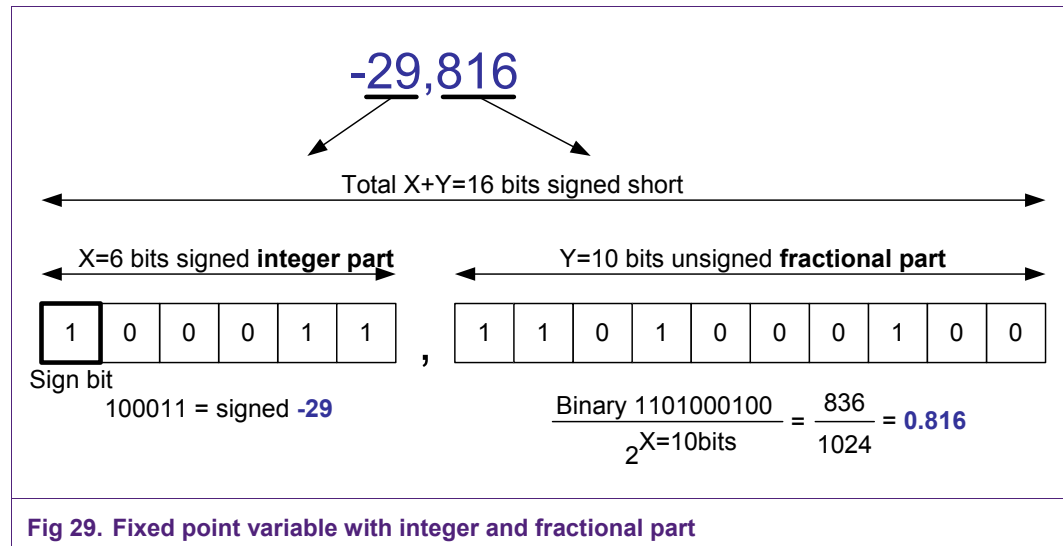


| | |
|----------------------|--|
| FOC board v1.3 | |
| 2009-10-29 05:08:44p | |
| Sheet: 3/3 | |

6. Appendix II: Fixed point

The easiest way to implement all the algorithms is to use floating-point variables. The LPC2900 however, has no hardware support for arithmetic with floating-point variables. All floating-point calculations are converted to integer instructions by the preprocessor and therefore would cause a high processor load. There alternative solution to calculate with fractional number without using floating-point is to use fixed-point variables.

With fixed-point variables the variable is split up into an integer part (X bits) and a fractional part (Y bits). The size of X+Y is the size of the total variable. If we take for example the total size of 16 bits of a signed short, we can divide it in two segments. The size of the integer part is 6 bits and the size of the fractional part is 10 bits.



The 6 bits integer part has a range from -32 to 31, and the fractional part has a range from 0 to 1023, which equals from 0 to 1023/1024 = 0.9990234.

The accuracy is 1/1024 = 0.0009765.

The advantage of using fixed-point variables is that the processor can perform integer math on fractional values without having to do the conversion of floating point math. Different integer and fractional sizes are used in various parts of the FOC software.

For the calculation of sine and cosine a lookup table with fixed-point values is used. Calculation of a fixed-point arctangent is done by CORDIC (COordinate Rotation Digital Computer) routines. CORDIC is an algorithm for the approximation of hyperbolic and trigonometric functions by rotating vectors in a unit circle.

7. Legal information

7.1 Definitions

Draft — The document is a draft version only. The content is still under internal review and subject to formal approval, which may result in modifications or additions. NXP Semiconductors does not give any representations or warranties as to the accuracy or completeness of information included herein and shall have no liability for the consequences of use of such information.

7.2 Disclaimers

General — Information in this document is believed to be accurate and reliable. However, NXP Semiconductors does not give any representations or warranties, expressed or implied, as to the accuracy or completeness of such information and shall have no liability for the consequences of use of such information.

Right to make changes — NXP Semiconductors reserves the right to make changes to information published in this document, including without limitation specifications and product descriptions, at any time and without notice. This document supersedes and replaces all information supplied prior to the publication hereof.

Suitability for use — NXP Semiconductors products are not designed, authorized or warranted to be suitable for use in medical, military, aircraft, space or life support equipment, nor in applications where failure or malfunction of a NXP Semiconductors product can reasonably be expected

to result in personal injury, death or severe property or environmental damage. NXP Semiconductors accepts no liability for inclusion and/or use of NXP Semiconductors products in such equipment or applications and therefore such inclusion and/or use is for the customer's own risk.

Applications — Applications that are described herein for any of these products are for illustrative purposes only. NXP Semiconductors makes no representation or warranty that such applications will be suitable for the specified use without further testing or modification.

Export control — This document as well as the item(s) described herein may be subject to export control regulations. Export might require a prior authorization from national authorities.

7.3 Trademarks

Notice: All referenced brands, product names, service names and trademarks are property of their respective owners.

8. Contents

| | | |
|-----------|--|-----------|
| 1. | Introduction | 3 |
| 2. | SVPWM..... | 5 |
| 2.1 | PMSM and BLDC difference | 5 |
| 2.2 | FOC basics | 5 |
| 2.3 | SVPWM..... | 8 |
| 2.4 | Duty cycle calculation..... | 11 |
| 2.5 | Current vector reconstruction | 14 |
| 2.6 | FOC overview | 15 |
| 3. | Sensorless FOC..... | 16 |
| 3.1 | Back-EMF principle | 16 |
| 3.2 | Slide Mode Controller..... | 18 |
| 3.3 | Phase compensation..... | 20 |
| 4. | Hard- and software..... | 21 |
| 4.1 | FOC Demoboard..... | 21 |
| 4.2 | Three phase inverter | 21 |
| 4.3 | DC-link current measurement | 22 |
| 4.4 | LPC2900 MSCSS | 23 |
| 4.5 | FOC demoboard additional features | 24 |
| 4.6 | Software..... | 25 |
| 4.7 | Dead time generation..... | 27 |
| 4.8 | Graphical user interface | 28 |
| 4.8.1 | Q&D PI controllers tab | 28 |
| 4.8.2 | Speed PID controller tab | 30 |
| 4.8.3 | SVPWM model tab..... | 30 |
| 4.8.4 | Virtual motor parameters tab..... | 31 |
| 4.8.5 | Open and save..... | 32 |
| 4.8.6 | Scope window | 32 |
| 4.8.7 | Datalogger..... | 32 |
| 5. | Appendix I: Hardware schematics | 33 |
| 6. | Appendix II: Fixed point..... | 36 |
| 7. | Legal information | 37 |
| 7.1 | Definitions | 37 |
| 7.2 | Disclaimers..... | 37 |
| 7.3 | Trademarks..... | 37 |
| 8. | Contents..... | 38 |

Please be aware that important notices concerning this document and the product(s) described herein, have been included in the section 'Legal information'.

© NXP B.V. 2009. All rights reserved.

For more information, please visit: <http://www.nxp.com>
 For sales office addresses, email to: salesaddresses@nxp.com

Date of release: 16 December 2009

Document identifier: AN10899_1

